



Doxycycline Adsorptive Interaction with Mesoporous MCM-41: Kinetic and Isotherm Modelling with Thermodynamics

Mukul Saxena^{1,2} · Jai Prakash Kushwaha³ · Shweta Kulshreshtha² · Gurleenjot Kaur⁴ · Neetu Singh³

Received: 4 March 2022 / Accepted: 17 April 2022 / Published online: 19 May 2022
© The Tunisian Chemical Society and Springer Nature Switzerland AG 2022, corrected publication 2022

Abstract

Antibiotics are bio-accumulating and persistent. its inappropriate disposal can affect human health and aquatic fauna. Development of antimicrobial resistance has been announced as one of the top ten threats to global health in 2019. In this study, Doxycycline adsorption on to MCM-41 (not reported earlier) was studied. Adsorbent dose (m), Doxycycline solution pH , adsorption time (t) and temperature (T) were considered as process parameters, and %Doxycycline removal and adsorption capacity were measured as responses of the adsorption. Parameters (m , pH and t) interaction, modelling and optimization for %Doxycycline removal and adsorption capacity was performed using Box Behnken Design. Based on this, a suitable model equation and adsorption mechanism was suggested. At optimized parameters, kinetics and adsorption rate controlling mechanism was studied. Further, various isotherm models (Freundlich, Langmuir and Redlich-Peterson) were studied to represent the adsorption equilibrium experimental data. the optimum process parameters were found to be $pH=7.3$, $m=0.02$ g/L and $t=20$ min. At optimized parameters, very high %Doxycycline removal of 99% with 2425 mg/g adsorption capacity was observed (max 835.5 mg/g adsorption capacity for Doxycycline is reported in literature). Thermodynamics study revealed enthalpy (ΔH°) = 23.02 kJ/mol confirming DCL physisorption on MCM-41.

Keywords Doxycycline · MCM-41 · Adsorption · Adsorption capacity · Antibiotics

1 Introduction

In recent years, high demand of antibiotics, triggered rapid development in pharmaceutical industries. According to a study, per capita use of Access antibiotics and Watch antibiotics increased by 26.2% and 90.9%, respectively [1]. Overall, 65% increase in antibiotics consumption and 39% increase in rate of antibiotic consumption has been reported [1–3].

Doxycycline (DCL) antibiotic belongs to the tetracycline family. It is used to treat infections related to wide range of gram-negative and gram-positive bacteria [4, 5]. It is also used effectively in viral infections like dengue and chikungunya. DCL has also been tried to effectively on COVID-19 + patients [6]. Nearly, 90% of the administered antibiotics is not absorbed/metabolised by the organisms and directly excreted in the environment [7]. Since, antibiotics are bio-accumulating and persistent in nature, inappropriate disposal of antibiotics by industries, wastewater treatment plants, hospitals etc. may adversely pollute water bodies. As a result, human health and aquatic fauna can be affected. Development of antimicrobial resistance has been

✉ Jai Prakash Kushwaha
jps_kag@yahoo.co.in

Mukul Saxena
mukul_ms@rediffmail.com

Shweta Kulshreshtha
shweta_kulshreshtha@rediffmail.com

Gurleenjot Kaur
gurleenswaich22@gmail.com

Neetu Singh
neetu.singh1479@gmail.com

¹ Department of Biotechnology, Institute of Engineering and Technology, Bundelkhand University, Jhansi, Uttar Pradesh, India

² Amity Institute of Biotechnology, Amity University Jaipur, NH-11C, Jaipur, Rajasthan, India

³ Department of Chemical Engineering, Thapar Institute of Engineering and Technology (Deemed to be University), Patiala, Punjab 147004, India

⁴ School of Energy and Environment, Thapar Institute of Engineering and Technology (Deemed to Be University), Patiala, Punjab 147004, India

announced as one of the top ten threats to global health in 2019, and it is increasing at an alarming rate [8]. Recently, DCL has been reported as one of the high-risk antibiotics towards aquatic [9–11].

Generally, biological and physicochemical methods are used for the treatment of water containing organic pollutants. Since, antibiotics are recalcitrant in nature, biological techniques are inefficient. Physicochemical methods such as electrochemical [12–14], advanced oxidation processes (AOPs) [15–19], and constructed wetland [20] has been reported for the treatment of water comprising DCL. The AOPs suffers with generation of transformed substrate to other organic compounds, with the complex operational conditions, high risk of hazardous chemicals involved and high cost [21]. However constructed wetland requires long time for treatment, very large area, and emits unpleasant odour.

Adsorption is widely popular and reliable technique with simpler operation, lower operational cost and high efficiency [4, 22–24]. Adsorption has been reported to be an important technique for the remediation of water comprising pharmaceutical compounds. Li et al. [25], Liang et al. [26] and Gao et al. [27] reported antibiotics adsorption with adsorption capacity of 1429 mg/g, 38.77 mg/g and 147.28 mg/g on to biochar, magnetic Fe₂O₃/biochar composite and biochar, respectively. Guo et al. [28] reported 625.9 mg/g adsorption capacity for antibiotic adsorption on to the Fe-MCM-41-A. A very good review was presented by the Aniagor et al. [4] for the adsorption of DCL on to various adsorbents. In this review, amongst other adsorbents, maximum 835.5 mg/g adsorption capacity towards doxycycline is reported for silica-based adsorbent (CoFe₂O₄/bio-silica nanocomposite) [29]. Therefore, research was focused on DCL adsorption on to silica based adsorbent capable of providing higher adsorption capacity. MCM-41 is silica based mesoporous adsorbent, which has been reported to exhibits very high surface with uniformly distributed pores, and admirable thermal/hydrothermal stability [30]. MCM-41 has been intensively investigated in the literature for different kind of pollutants adsorption [31]. Further, doxycycline adsorption on various other adsorbents have also been studied and reported [4]. To the best of authors knowledge, no study in literature is available for the doxycycline (DCL) adsorption on to MCM-41.

In the present study, DCL adsorption on to MCM-41 was studied. Adsorbent dose (m : 0.02–0.4 mL), DCL aqueous solution pH : 2–10, adsorption time (t : 30–210 min) and temperature (T : 288–318 K) were considered as process parameters, and %DCL removal (%D_R) and adsorption capacity (Q : mg/g) were measured as responses of the adsorption. Process parameters (m , pH and t) interaction, modelling and optimization for responses %D_R and Q was performed using Box Behnken (BB) design. Based on the behaviour of adsorption with the parameters, suitable adsorption mechanism was suggested. At optimized parameters, kinetics and

diffusion of DCL adsorption was studied. Further, various isotherm models (Freundlich, Langmuir and Redlich-Peterson) were tested to validate the experimental adsorption equilibrium data. Thermodynamics study was also performed and variation in Gibbs energy (ΔG_0), entropy (ΔS_0) and enthalpy (ΔH_0) were calculated for adsorption at different temperatures.

2 Materials and Methods

2.1 Chemicals and Adsorbent

Cetyl trimethyl ammonium bromide surfactant and Tetraethyl Orthosilicate silica source was purchased from Sigma-Aldrich. Doxycycline hydrochloride antibiotic was supplied by a pharmaceutical industry situated in Baddi, HP, India. Further, Sodium Hydroxide and Hydrochloric acid were provided by Loba chemie, Mumbai, India.

In this study, silica based MCM-41 adsorbent was synthesized with the help of Cetyl trimethyl ammonium bromide surfactant and Tetraethyl Orthosilicate silica source using hydrothermal root [24, 32]. The prepared adsorbent was characterized for its surface area, pore size and volume using Multipoint Brunauer-Emmett-Teller (BET: BELSORP mini-II, Japan), structure and crystallinity with XRD (X-ray powder diffractometer; Philips, Netherlands), functional groups on surface with Fourier Transform Infrared spectrometer (FTIR: in 500–4000 cm⁻¹; Resolution Pro Carry 660, Agilent Technologies) and morphology using Scanning Electron Microscopy (FE-SEM: Hitachi X-650, Japan) and High Resolution Transmission Electron Microscopy; (HR-TEM: Tecnai G2 20, FEI, US).

Detailed characteristics results, graphs and figures have already been published elsewhere [23, 24]. However, herein main characteristics is presented. BET analysis revealed 502.77 m²/g surface area of prepared adsorbent MCM-41. Further, BET average pore diameter of 3.21 nm confirms the meso-porosity of the prepared adsorbent (meso-pores: 20 Å < d < 500 Å) with 0.85 cm³/g pore volume. Low-angled XRD (2 θ : 0°–10°) exposed a broad but not intense peak at 0.98° due to the hexagonal pores, which confirmed the amorphous nature of prepared MCM-41. HR-TEM confirmed the hexagonal shape of MCM-41.

2.2 Adsorption Experiments and Analysis

In present study, adsorption experiments of DCL from aqueous solution on to MCM-41 were designed, conducted and analysed as per the Box Behnken (BB) Design of design expert 6.0 under response surface methodology (RSM). RSM, a well-known tool reinforced with statistical and mathematical techniques, is useful for optimization, analysis

and modelling of problems where response/responses of a process is related to a number of parameters and in more complex situation there is interaction between the parameters [33, 34]. BB design is a rotatable/nearly rotatable revolving design observed as a cube. It is second order design based on the three-level incomplete factorial design. BB design levels special configuration permits the number of design points to increase at the same rate as the number of polynomial coefficients [35]. The adsorption process parameters (pH: 2–10; m: 0.02–0.21 g/L and t: 30–210 min) with three levels were selected experimental design using BB design, while %DCL removal (%D_R) and adsorption capacity (Q) has been selected the responses of the process. Total 17 experiments was suggested by the BB design, and the design matrix is shown in Table 1.

In order to conduct the experiments in batch mode, DCL stock aqueous solution of 1000 mg/L was prepared in double distilled water, and required aqueous DCL solutions for the experiments were obtained from its dilution. To conduct the experiment, 50 ml of DCL solution of 50 mg/L concentration with suitable amount of adsorbent MCM-41 was taken in 100 ml conical flask. In each such experiments, the adsorption process parameters such as pH of DCL solution, dose of adsorbent MCM-41 and the adsorption time was fixed as per the experimental condition (Table 1). To alter the DCL solution pH, 0.1 N HCl and NaOH solutions were used. The adsorption process was started by placing the flask in a temperature-controlled incubator shaker (Remi Elektronik Ltd., India; CIS 24 Plus) at 180 rpm and 298 K. At the end of the experiment, the flask was removed, and adsorbent MCM-41 was separated from the DCL solution

using syringe filter. Then after, residual DCL concentration was analysed using UV–Vis spectro-photometer (double beam Prekin Elmer Lambda 35) at $\lambda_{\max} = 345$ nm. Further, % DCL removal (%D_R) and MCM-41 adsorption capacity (Q) was calculated using Eqs. 1 and 2.

$$\%D_R = \frac{(C_0 - C_f)100}{C_0} \quad (1)$$

$$Q = \frac{(C_0 - C_f)}{m} V \quad (2)$$

In the above Eqs. 1 and 2, C₀: Initial DCL concentration at the start of adsorption experiment (mg/L); C_f: Final DCL residual concentration in the solution (mg/L).

The obtained experimental responses of the DCL-MCM-41 adsorption system (%D_R and Q) were then processed for second order polynomial equation (Eq. 3) to explore the interaction between the process parameters and responses.

$$Y = A + \sum_{i=1}^k A_i X_i + \sum_{i=1}^k A_{ii} X_i^2 + \sum_{i < j} A_{ij} X_i X_j + E \quad (3)$$

where, Y: System response; A: coefficient; X_i, X_i² and X_iX_j: independent, square and interaction effects of process parameters, respectively; A_i, A_{ii} and A_{ij}: coefficients; E: Error value.

The validation quality of second order polynomial model was accessed through non-linear regression and by determining coefficient of determination R² and adjusted and

Table 1 Box Behnken experimental design matrix with actual and predicted values of responses for the DCL adsorption on to MCM-41

Std	pH	t (min)	m (g/L)	(%D _R) (Actual)	(%D _R) (Predicted)	Q (mg/g) (Actual)	Q (mg/g) (Predicted)
1	2	30	0.21	81.46	82.07	193.96	151.32
2	10	30	0.21	99.00	99.45	235.72	296.04
3	2	210	0.21	80.13	79.69	190.79	130.48
4	10	210	0.21	97.87	97.27	233.03	275.67
5	2	120	0.02	78.84	78.73	1970.93	2061.62
6	10	120	0.02	97.89	97.94	2447.26	2435.00
7	2	120	0.4	82.72	82.67	103.41	115.66
8	10	120	0.4	98.31	98.42	122.88	32.19
9	6	30	0.02	96.41	95.92	2410.30	2362.24
10	6	210	0.02	93.54	94.09	2338.46	2308.08
11	6	30	0.4	99.14	98.58	123.92	154.30
12	6	210	0.4	95.35	95.85	119.19	167.24
13	6	120	0.21	95.48	95.57	227.34	227.54
14	6	120	0.21	95.68	95.57	227.81	227.54
15	6	120	0.21	95.55	95.57	227.50	227.54
16	6	120	0.21	95.51	95.57	227.42	227.54
17	6	120	0.21	95.61	95.57	227.65	227.54

predicted R^2 values. Further, desirability function of Design Expert 6.0 was applied in order to simultaneous optimization of responses $\%D_R$ and adsorption capacity (Q). Here desirability of each of the response $\%D_R$ and Q together combined for an overall desirability to find the best maximum of response [35, 36].

3 Results and Discussion

3.1 Statistical Analysis and Model Fitting

The experiments suggested by the BB design (Table 1) were conducted, and obtained responses correlation with the process parameters were estimated by fitting the experimental data for ANOVA to the quadratic model (Eq. 5). Further, the experimental data were also used to estimate the model significance, model terms and interactions between the process parameters. The quadratic model F-value of 272.14 and 311.38 for the responses $\%D_R$ and Q, respectively, with p-value < 0.0001 signifies that the experimental data best represented by the quadratic model (Table 2). For Prob > F value less than 0.05 for any model term, the corresponding model term is significant under the 95% confidence level. In this case, pH , t , m , pH^2 and $pH \times m$, and pH , m , m^2 and $pH \times m$ are the significant term for the responses $\%D_R$ and Q, respectively. The suggested quadratic model for responses $\%D_R$ and Q with their coefficient and independent, square and interaction effects of process parameters are represented by the Eqs. 4 and 5.

$$\begin{aligned} \% \text{ Removal } (\%D_R) = & 67.75 + 7.14pH - 0.0213t \\ & + 12.16m - 0.394pH^2 + 0.000044t^2 \\ & + 5.016m^2 + 0.00014(pH \times t) \\ & - 1.142(pH \times m) - 0.0134(t \times m) \end{aligned} \quad (4)$$

$$\begin{aligned} \text{Adsorption Capacity (Q, mg/g)} \\ = & 2322.93 + 87.52pH - 1.40t - 16387.29m \\ & - 3.16pH^2 + 0.0045t^2 + 27259.91m^2 \\ & + 0.0003.3(pH \times t) - 150.28(pH \times m) \\ & + 0.98(t \times m) \end{aligned} \quad (5)$$

The adequate precision, a measure of signal to noise ratio, was found 47.204 and 44.87 for the responses $\%D_R$ and Q, respectively, signifying the models can be used to navigate the design space and hence optimization. Further, the validation quality of experimental data to the models were also justified by the high coefficient of determination (R^2) values 0.997 ($\%D_R$) and 0.99 (Q). This indicates that only 0.3% and 0.1% of the total variations were impenetrable by the quadratic model for responses $\%D_R$ and Q, respectively. Moreover, adjusted R^2 and predicted R^2 values were found to be, 0.99, 0.95 for $\%D_R$ and, 0.99, 0.96 for Q, which also advocates the validity of the model. The reproducibility of the responses is indicated by the CV values, which was found to be 0.62 and 10.21 indicating higher reproducibility [37]. Normal % probability versus studentized residuals (Fig. 1), and predicted versus actual values plots (Fig. 2) for responses $\%D_R$ and Q also proved the capability and accuracy of the quadratic models.

Table 2 ANOVA of the responses $\%D_R$ and adsorption capacity (Q: mg/g) for DCL removal on to MCM-41

Source	$\%D_R$					Q (mg/g)				
	Sum of squares	DF	Mean square	F-value	Prob > F	Sum of squares	DF	Mean square	F-value	Prob > F
Model	802.17	9	89.13	272.14	<0.0001	1.36×10^7	9	1.5×10^6	311.38	<0.0001
A	611.05	1	611.05	1865.695	<0.0001	42,022.65	1	42,022.65	8.619	0.0218
B	10.40	1	10.40	31.742	0.0008	849.3706	1	849.3706	0.174	0.6889
C	9.76	1	9.76	29.806	0.0009	9.46×10^5	1	9.46×10^5	1939.543	<0.0001
A ²	167.64	1	167.64	511.839	<0.0001	10,740.66	1	10,740.66	2.203	0.1813
B ²	0.54	1	0.54	1.663	0.2382	5560.229	1	5560.229	1.140	0.3210
C ²	0.14	1	0.14	0.421	0.5369	4.07×10^6	1	4.07×10^6	836.363	<0.0001
AB	0.01	1	0.01	0.030	0.8667	0.056313	1	0.056313	1.1×10^{-5}	0.9974
AC	3.01	1	3.01	9.200	0.0190	52,178.47	1	52,178.47	10.703	0.0136
BC	0.21	1	0.21	0.637	0.4510	1125.926	1	1125.926	0.231	0.6455
Residual	2.29	7	0.33			34,127.35	7	4875.335		
Lack of Fit	2.27	3	0.76	118.042	0.0002	34,127.2	3	11,375.73	3.13×10^6	<0.0001
Pure Error	0.03	4	0.01			0.145163	4	0.036291		
Cor Total	804.46	16				1.36×10^7	16			

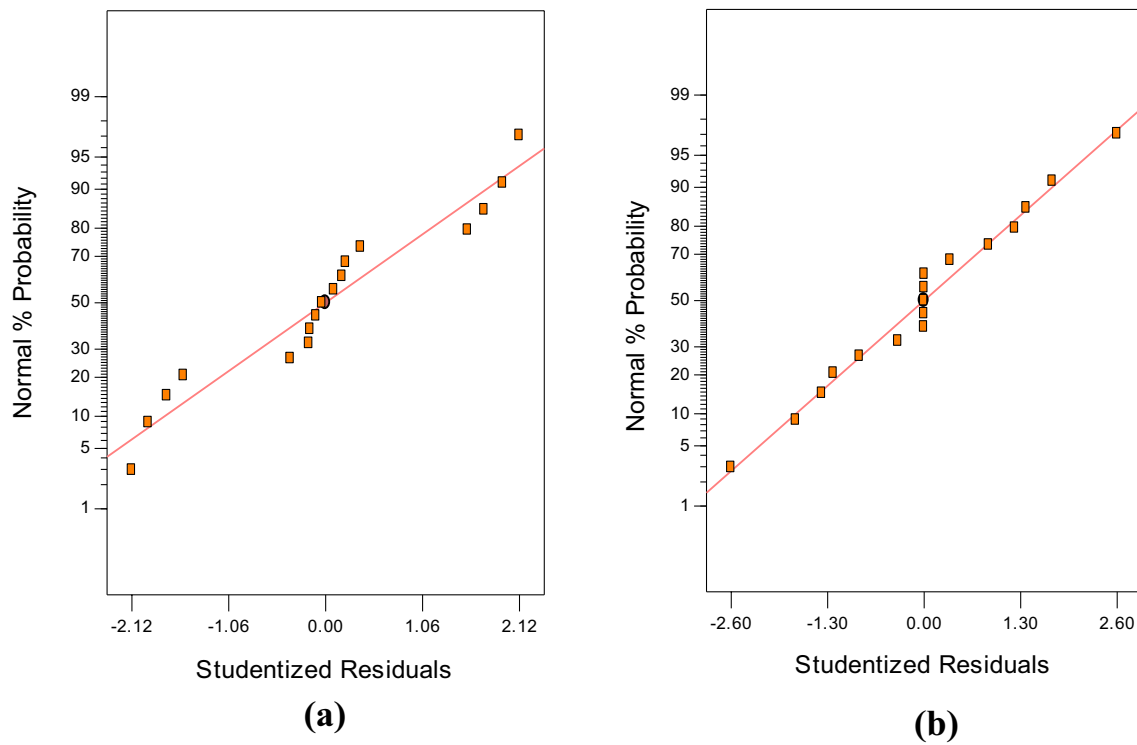


Fig. 1 Normal % probability versus studentized residuals plots for responses **a** % removal ($\%D_R$) **b** adsorption capacity (Q)

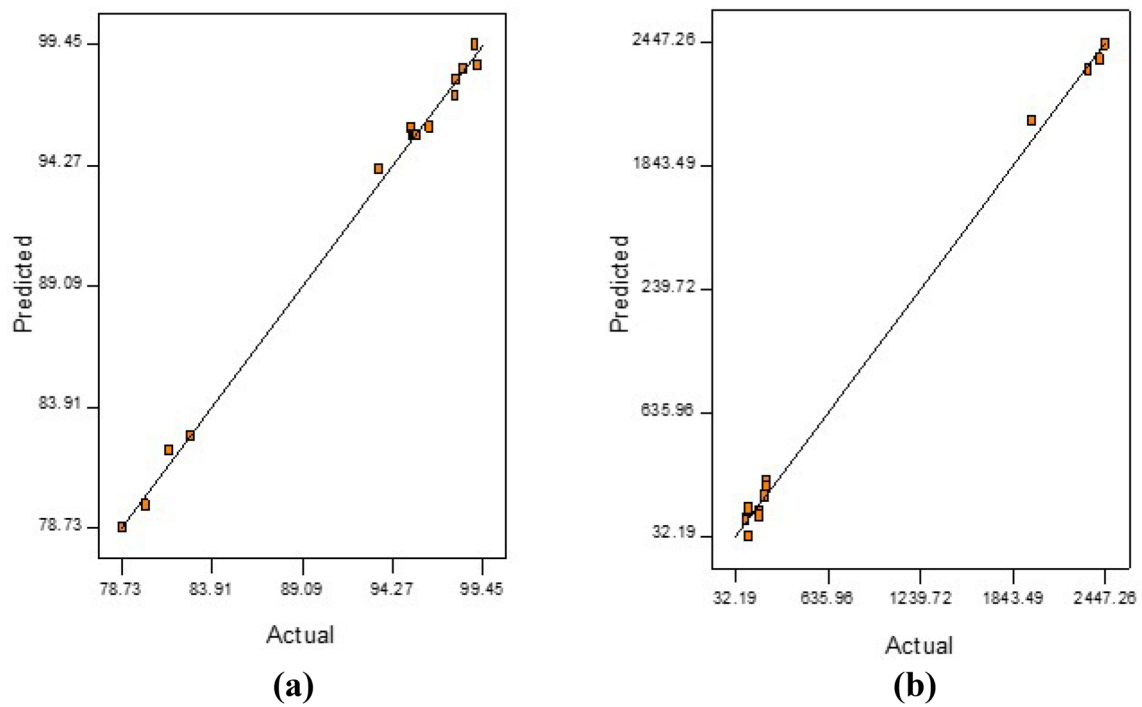


Fig. 2 Predicted versus actual plot for responses **a** % removal ($\%D_R$) **b** adsorption capacity (Q)

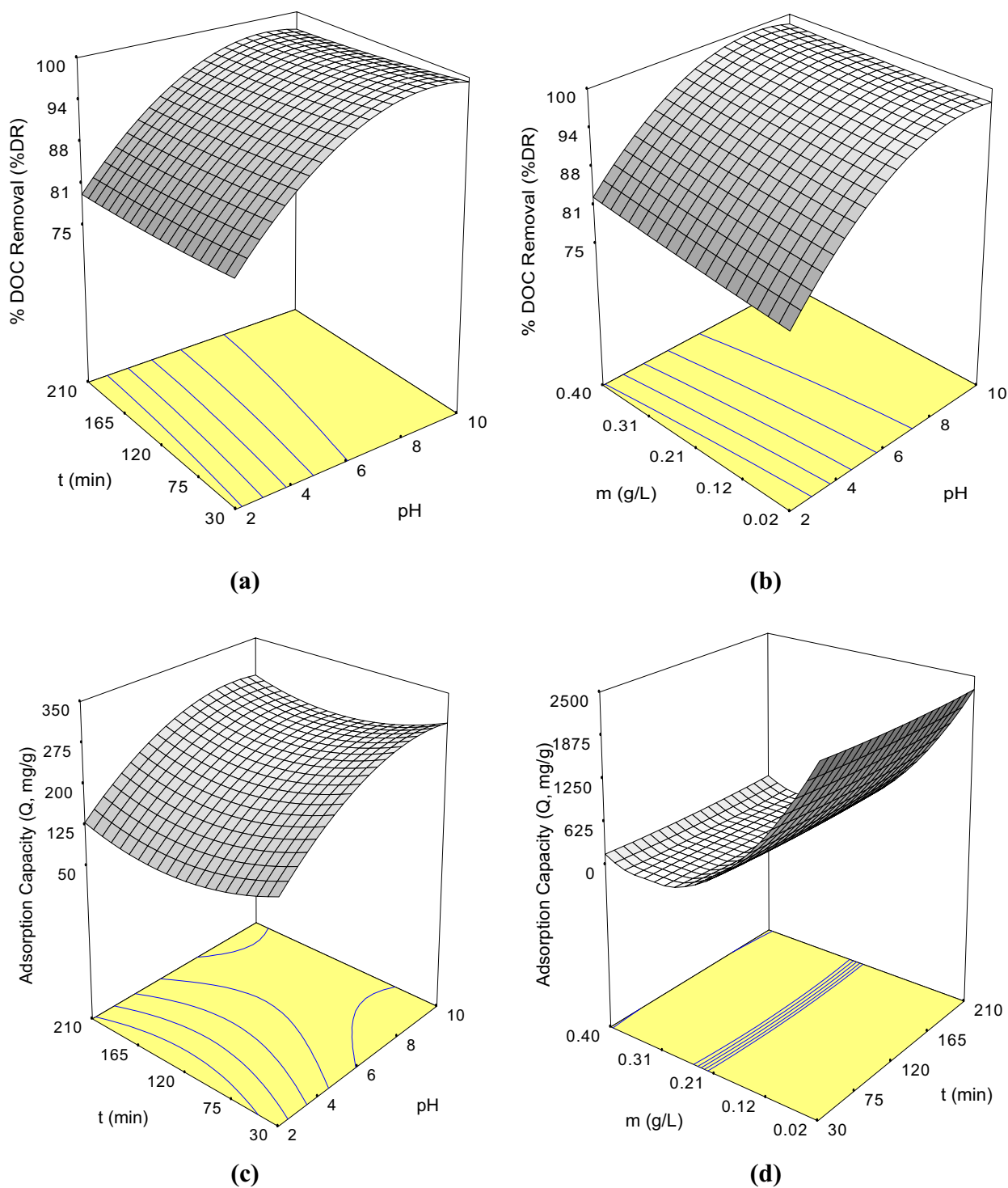


Fig. 3 3-D response surface graph showing the interaction within parameters for %DCL removal (a, b) and adsorption capacity (c, d)

3.2 Effect of Process Parameters and Optimization

Process parameters (pH , dose: m and adsorption time: t) individual and interactive effects on the responses % D_R and Q is described by the 3-D response surface plots

(Fig. 3). The interactive effect of pH and t can be seen in Fig. 3a. It can be observed that with increase in pH , the % D_R is increasing. Maximum % D_R can be observed at $pH \approx 7.8$, and for all $pH > 7.8$, the % D_R starts decreasing. This variation in % D_R with pH can be observed true at all the

t values. However, at any pH , there is nearly no change in $\%D_R$ value with the change in t value. This concludes that the maximum of the DCL is adsorbed on the MCM-41 at initial time of adsorption, and is an indication of high efficacy of the adsorbent MCM-41. Figure 3b shows the interactive effect of pH with adsorbent dose m on $\%D_R$. Same behaviour can be seen with change in pH on $\%D_R$, as it was observed in Fig. 3a. Whereas, with change in m value the $\%D_R$ was found increasing at all the pH values. However, the $\%D_R$ rate of increase with m is higher at low pH . This may be due to fact that higher pH is supporting the adsorption of DCL on MCM-41, and maximum available DCL in the solution is adsorbed at lower value of adsorbent dose m . At lower pH , which is not favouring the adsorption of DCL, increasing m provides higher active surface for the adsorption and hence, adsorption of DCL is increased.

Figure 3c shows the interactive effect of pH with adsorption time t on adsorption capacity (Q). It can be observed that with increase in pH , the Q value is increasing showing its maximum at $pH \approx 7.8$. At all $pH > 7.8$, the Q starts decreasing. This trend in Q variation with pH was observed at all the t values. However, at any pH , there is slight variation (practically no change) in Q value with the change in t value. This also indicates the high efficacy of the adsorbent MCM-41. In Fig. 3d, Interactive effect of adsorption time (t) and dose (m) is shown. It can be observed that at any value of t , increased m value up to $m \approx 0.31$ g/L decreases the Q value. For all $m > 0.31$ mg/L, the Q value becomes constant. This also indicates the high efficacy of the MCM-41, as high Q was observed at lower m value due to high adsorption of available DCL in the solution. Increased m value did not improve the Q in spite decreased it.

For the optimization of operating parameters of the MCM-41 and DCL adsorption system, simultaneous multiple response optimization of $\%D_R$ and Q of design expert 6.0 was followed. For this purpose, process parameters m and t were set within their entire range of study, while pH was set targeted to 7.3. The DCL solution original pH is ≈ 7.3 , and Fig. 3a–c revealed that there is no significant change in responses $\%D_R$ and Q after $pH = 7.5$. Therefore, in order to save the chemical cost to alter the pH , the pH was set targeted to 7.3 during the optimization. The optimization process was conducted to maximize both the responses, $\%D_R$ and Q . Further, minimum and maximum adequacy of the responses, $\%D_R$ and Q , individual and simultaneous desirability was accessed. The individual desirability for both $\%D_R$ and Q was 1.0, however, overall desirability was 0.719. Under this desirability, the optimum adsorption process parameters for DCL and MCM-41 system were found to be $pH = 7.3$, $m = 0.02$ g/L and $t = 20$ min, and responses $\%D_R$ and Q was predicted to be 99% and 2425 mg/g, respectively. In order to validate the optimization result, three

experiments were conducted at the optimized parameters ($pH = 7.3$, $m = 0.02$ g/L and $t = 20$ min), and the average values of measured responses $\%D_R$ and Q were, 98% and 2510 mg/g, respectively. The very closer experimental responses to predicted responses proves the adequacy of the suggested quadratic model and optimized parameters by the BB design.

3.3 Mechanism

The mechanism of adsorption of DCL from aqueous solution on to MCM-41 can be explained on the basis of MCM-41 surface charge and ionisation state of DCL molecules with the change in the pH of DCL solution. There are three dissociation constant values ($pK_{a1} = 3.02$, $pK_{a2} = 7.97$ and $pK_{a3} = 9.15$) for DCL molecule. Therefore, it turns to be positively charged i.e. in cation for $pH < pK_{a1}$ (3.02), zwitterionic in the pH range $3.02 < pH < 7.97$ ($pK_{a2} = 7.97$) and anionic in the $7.97 < pH < 9.15$ and $pH > 9.15$ ($pK_{a3} = 9.15$) [38].

The MCM-41 surface behaves as the negatively charged surface due to the presence of Si and the hydroxylated silica group (Si–OH) on the surface (as described by the FTIR spectra in Sect. 2.1). Further, the surface negativity of the MCM-41 surface is increased by the increasing pH as the point of zero charge (pH_{PZC}) for hydroxylated surface of silica is about 2, and the pK_a of Si–OH group on the MCM-41 surface is 6.5 [39].

In the present study, increasing pH from highly acidic pH to $pH \approx 7.8$ revealed increase in both the responses $\%D_R$ and Q . For all $pH > \approx 7.8$ to, the $\%D_R$ and Q starts decreasing (Fig. 3). The optimization analysis performed in the above paragraph (Sect. 3.2) concluded the optimum pH being 7.3 at which maximum $\%D_R$ and Q : 99% and 2425 mg/g, respectively, were observed. In this pH range (from highly acidic to $pH \approx 7.8$) the DCL molecules turn to zwitterion from cation, and the MCM-41 surface becomes more anionic. In this situation the physical interactions like hydrogen bonds between –OH and –H of DCL–MCM-41 adsorption system may be the probable mechanism of higher adsorption of DCL on MCM-41 surface (Fig. 4). Further, in zwitterionic form, the DCL solubility in water becomes low. This leads to hydrophobic interaction [38] of DCL with MCM-41 surface enhancing the $\%D_R$ and Q . At highly acidic pH , both the MCM-41 surface and DCL molecule turns to be positively charged, and high electrostatic repulsion reduced the adsorption. However, at highly basic pH ($pH > 9.15$), both the MCM-41 surface and the DCL molecules turns to be anionic, and electrostatic repulsion is the reason of decreasing $\%D_R$ and Q .

FTIR spectra of fresh and loaded MCM-41 is shown in (Fig. 5) peaks at 1057 cm^{-1} confirming stretching vibrations of Si–O–Si on the surface. Another peak at 961 cm^{-1}

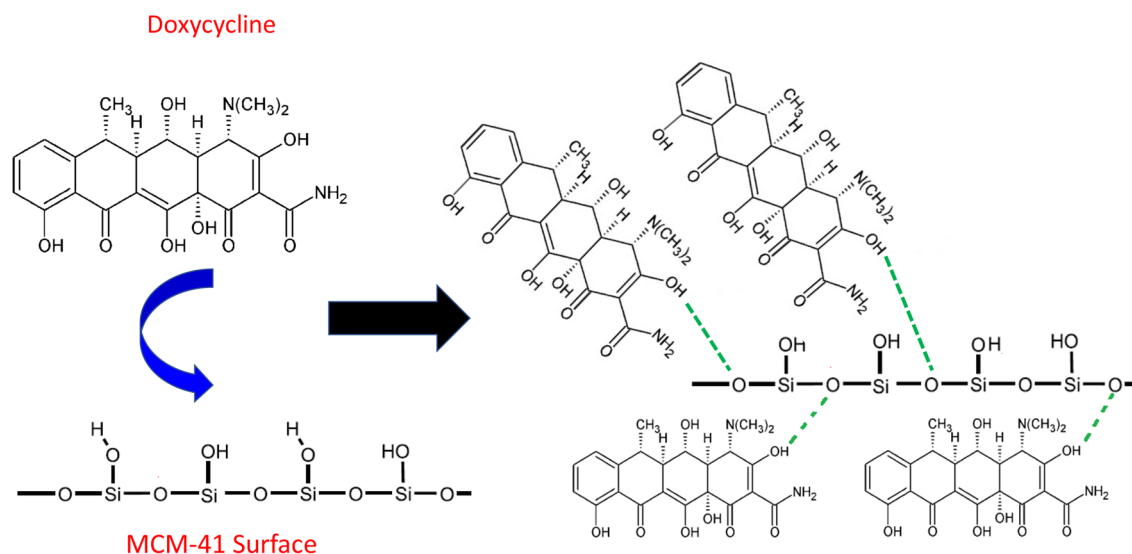


Fig. 4 Proposed mechanism for DCL adsorption on MCM-41 surface

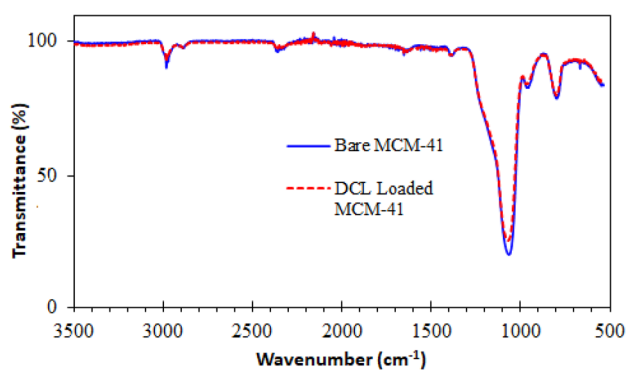


Fig. 5 FTIR spectra of fresh and DCL loaded MCM-41

represented Si–OH vibrations. Peak at 797 cm^{-1} verified the presence of silica on the MCM-41 surface. Vibration of –OH is confirmed by the peaks at $2900\text{--}3100\text{ cm}^{-1}$. No noticeable changes were observed in the FTIR spectra after the adsorption of DCL. The new functional groups in the FTIR spectra may appear due to covalent modifications in the MCM-41 after the adsorption. However, if there is non-covalent interaction (like hydrogen bonding which is strong non-covalent interaction)/van der Waals physical interaction, slight peak shift or slight reduction in peak intensities without change in peak position takes place [23, 40–42]. In the present study, very small reduction in peak intensities were

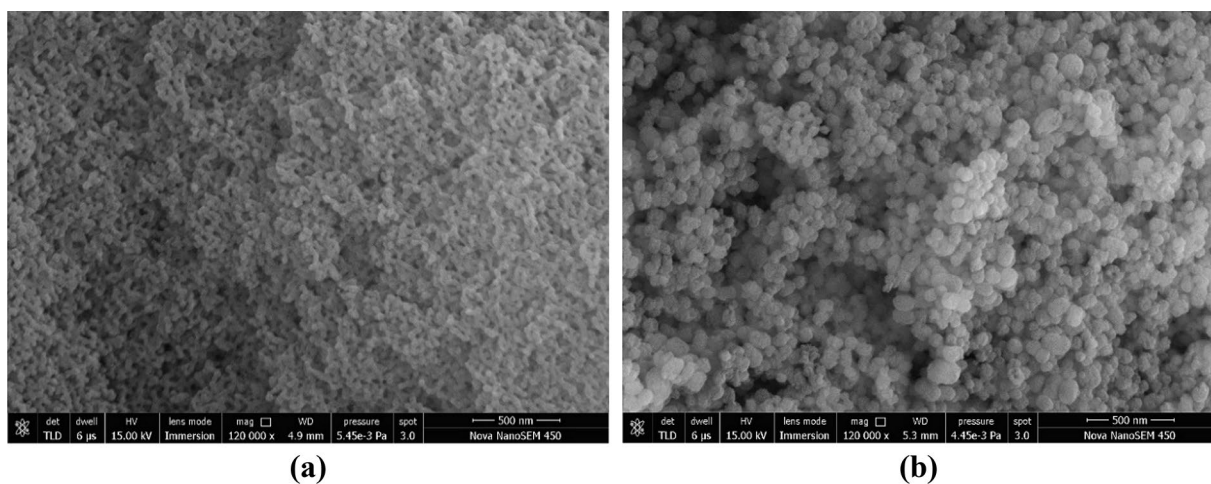


Fig. 6 SEM **a** fresh and **b** DCL loaded MCM-41

observed confirming the non-covalent interaction (hydrogen bonding) of DCL with MCM-41.

The DCL adsorption can also be evident from the SEM micrograph (Fig. 6) and EDX result. The elemental analysis (EDX) discovered presence of Si and O (wt%) by 69.03% and 30.97%, respectively. While for DCL loaded MCM-41, revealed Si, O and C by 59.23%, 34.16% and 6.61%, respectively.

3.4 Kinetics and Diffusion

Adsorption kinetics of DCL on to MCM-41 was studied by validating the experimental data collected using non-linear regression method. For this purpose, pseudo-first-order (Eq. 6) and pseudo second-order (Eq. 7) kinetic model was applied [43–45].

$$Q_t = Q_e [1 - \exp(-k_f t)] \quad (6)$$

where, k_f is the pseudo-first-order rate constant.

$$Q_t = \frac{tk_s Q_e^2}{1 + tk_s Q_e} \quad (7)$$

The initial adsorption rate, h (mg/g min), at $t \rightarrow 0$ is defined as:

$$h = k_s Q_e^2 \quad (8)$$

where, Q_t : DCL quantity adsorbed on MCM-41 Surface (mg/g) at any time (t); k_f and k_s : Rate constant for pseudo first-order and pseudo second-order kinetics.

For the non-linear regression and to find best suitable kinetic model, MPSD (Marquardt's percent standard deviation) objective function (error function) was applied (Eq. 9)

$$MPSD = 100 \sqrt{\frac{1}{n_m - n_p} \sum_{i=1}^n \left(\frac{q_{t,i,exp} - q_{t,i,cal}}{q_{t,i,exp}} \right)^2} \quad (9)$$

where, exp and cal are the experimental data and calculated data values; n_m and n_p are the data measurements and parameters in the model, respectively.

To collect the experimental data, DCL aqueous solution of different concentrations (C_0 : 25, 50 and 100 mg/L) were kept in contact with the MCM-41 at optimized parameters ($pH = 7.3$ and $m = 0.02$ g/L) for 60 min.

In Fig. 7, very fast DCL adsorption can be observed within 5 min of adsorption on to MCM-41 followed by a slower adsorption period. This fast DCL adsorption can be attributed to the adsorption onto the ample vacant sites of the MCM-41. After 20 min of DCL adsorption, the adsorption rate becomes constant due to the lesser availability of sites and diffusion to the inner surface of MCM-41 pore

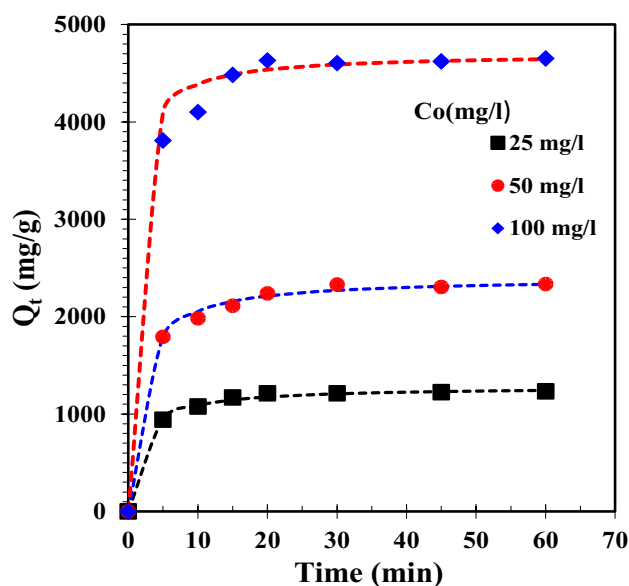


Fig. 7 Kinetics of DCL on MCM-41 at optimized parameters ($m = 0.02$ g/L and $pH = 7.3$) (Data points shows experimental results and Solid line shows pseudo second-order kinetic model fitting)

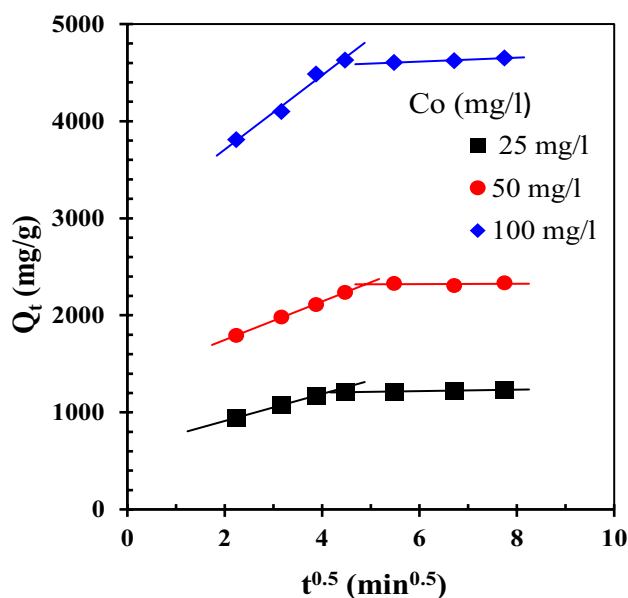
[46]. This trend of DCL adsorption was observed at all the C_0 values.

The coefficient of determination (R^2), MPSD values with the model parameters values for the best fitted experimental data to the kinetic models are given in Table 3, and fitting is shown in the Fig. 7. In Table 3, it can be seen that the coefficient of determination (R^2) values is very high (≈ 0.99) for both the pseudo first-order and pseudo second-order models at all the $C_0 = 25, 50$ and 100 mg/L. However, the MPSD error values are much smaller at all the C_0 values for the pseudo second-order kinetic model. This concludes the pseudo second-order kinetic model is best suitably representing the adsorption kinetics of DCL on to MCM-41 surface. It can also be observed from Table 3 that h (mg/g min) and Q_e values increases with increase C_0 values. The Rate constant values for pseudo second-order kinetics (k_s) were observed decreasing with increasing C_0 . The values of h and Q_e and their increasing trend with C_0 concludes the adsorption is limited by the limiting C_0 of DCL in the solution indicating high adsorption capacity of the MCM-41. Actually, the increased C_0 value increases the driving force, which ultimately increases the interaction and hence mass transfer between DCL molecules and MCM-41 surface leading to increased adsorption.

Since, adsorption process involves a number of steps (external film diffusion, intra-particle or pore diffusion and adsorption on pore surface), and pseudo-first-order/pseudo second-order kinetic models do not provide the information about the slowest/controlling steps and diffusivity. This study was conducted ensuring well mixing of

Table 3 Kinetic parameters DCL adsorption on to MCM-41 at optimized parameters ($pH=7.3$ and $m=0.02$ g/L, $t=60$ min)

Pseudo-first-order model					
C_o (mg/l)	$Q_{e,exp}$ (mg/g)	$Q_{e,cal}$ (mg/g)	k_f (min^{-1})	R^2	MPSD
25	1233.39	1221.69	0.37	0.99	10.01
50	2335.13	2287.11	0.31	0.99	8.96
100	4651.16	4629.99	0.22	0.99	1.09
Pseudo-second-order model					
C_o (mg/l)	$Q_{e,cal}$ (mg/g)	k_s (g/mg min)	h (g/mg min)	R^2	MPSD
25	1279.81	0.00044	715.72	0.99	2.97
50	2397.58	0.00025	1422.62	0.99	3.60
100	4722.0	0.00023	6480.46	0.99	3.31

**Fig. 8** Weber-Morris plot for the adsorption of doxycycline on to MCM-41 ($m=0.02$ g/L and $pH=7.3$, $t=60$ min). (Data points shows experimental results and Solid line shows pseudo second-order kinetic model fitting)

adsorbate-adsorbent system avoiding the external film diffusion. Therefore, to expose the slowest/controlling step the intra-particle diffusion model (Eq. 10) [47, 48] was studied.

$$Q_t = Kt^{1/2} + C \quad (10)$$

where, K ($\text{mg/g min}^{1/2}$): Intra-particle diffusion rate constant and C : boundary layer thickness indicator.

Multilinear plot of Q_t Vs $t^{0.5}$ for DCL adsorption on MCM-41 can be observed. If the intra-particle pore diffusion is rate controlling, then Q_t Vs $t^{0.5}$ plot should be linear passing through origin. However, more than one linear plot (Q_t Vs $t^{0.5}$) in present study (Fig. 8) indicates involvement of other steps as rate controlling step except intra-particle pore diffusion.

External mass transfer, in the present study, is very fast due to assured well mixing. Therefore, intra-particle pore diffusion, which can be represented by first linear plot (Fig. 8) representing the gradual approach towards the DCL adsorption equilibrium, may be concluded as rate limiting step [47]. However, the second linear part explains the final equilibrium of DCL adsorption on to MCM-41. The slopes (rate constants) of these linear portions K_1 and K_2 for different C_o values are depicted in Table 4. The rate constant of first linear portion is higher than second linear part describing the higher adsorption due to high DCL concentration and hence higher driving force.

Therefore, whether the surface diffusion is rate limiting, kinetic experimental data of DCL adsorption to MCM-41 were applied to Boyd kinetic model (equation 11) [49].

Table 4 Weber-Morris intra-particle diffusion model for the adsorption of doxycycline on to MCM-41 ($m=0.02$ g/L and $pH=7.3$, $t=60$ min)

C_o (mg/L)	K_1 ($\text{mg/g min}^{1/2}$)	C_1 (mg/g)	R^2	K_2 ($\text{mg/g min}^{1/2}$)	C_2 (mg/g)	R^2
25	139.82	631.58	0.99	5.22	1193	0.93
50	197.48	1353.7	0.99	18.34	2312.2	0.97
100	383.21	2939.80	0.98	20.10	4492.40	0.96

$$F = 1 - \frac{6}{\pi^2} \exp(-B_t) \quad (11)$$

or

$$B_t = -0.4977 - \ln(1 - F) \quad (12)$$

where, $F = Q_t/Q_e$ and B_t is a function of F .

The B_t Vs t plot should be linear and passes through origin if the intra-particle diffusion is rate limiting. In the present study, the B_t versus t (not provided here) was observed non-linear showing R^2 in the range of 0.62–0.86 for the DCL concentration study range. Therefore, it may be concluded that the intra-particle diffusion does not represent the sole rate limiting step, but the surface diffusion is also limiting the DCL adsorption on MCM-41.

3.5 Isotherm Modelling and Thermodynamics

The variation in the DCL adsorption capacity (Q_e) with the change in DCL concentration (C_0 ; 10–100 mg/L) was studied at different temperature (288–318 K) and at optimum adsorption parameters ($pH = 7.3$, $m = 0.02$ g/L and $t = 20$ min). The experimental data collected were validated to different isotherm models: Freundlich, Langmuir and Redlich and Peterson (R-P) isotherms, using non-linear regression [50] with CHI^2 error function. The fitting of experimental data is shown in Fig. 9, and the isotherms parameters calculated are represented in Table 5.

It can be observed that, the C_e value is decreasing and hence Q_e is increasing with increase in temperature (T) at all the DCL C_0 studied (Fig. 9). Therefore, the DCL adsorption on the MCM-41 is endothermic. Generally, endothermic nature of adsorption is due to if intra-particle diffusion is rate limiting, as

Fig. 9 Isotherms at different temperature for the adsorption of doxycycline on to MCM-41. Symbols represents the experimental data and the lines predicated by the isotherms. **a** Freundlich Isotherm. **b** Langmuir isotherm. **c** R–P isotherm

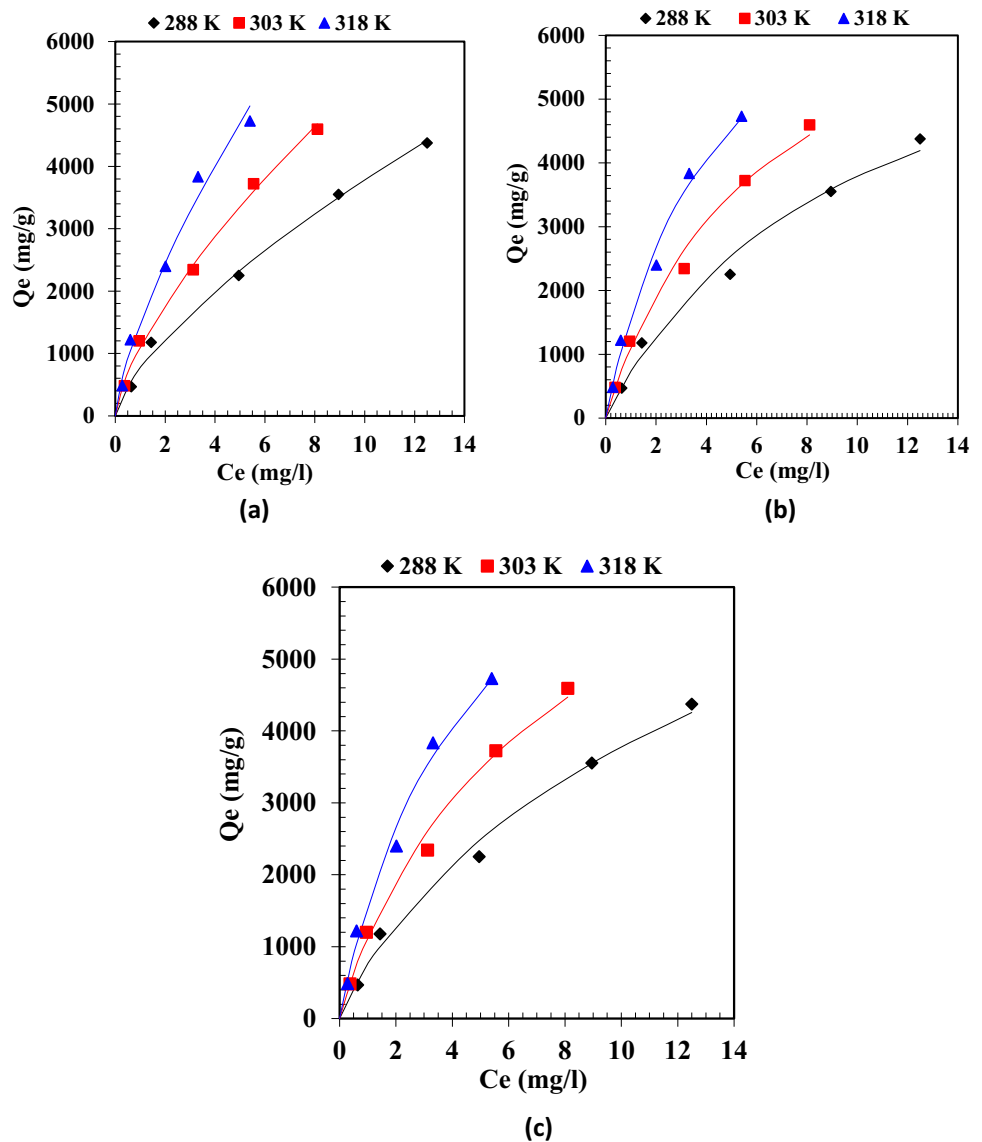


Table 5 Isotherm models and Thermodynamic parameters for the adsorption of doxycycline on to MCM-41 ($m=0.02$ g/L and $pH=7.3$, $t=20$ min)

Freundlich					
		$Q_e = K_F C_e^{1/n}$			
T (K)	$K_F ((\text{mg/g})/(\text{l/mg})^{1/n})$	$1/n$	R^2	CHI2	
288 K	759.58	0.697	0.99	53.2	
303 K	1100.3	0.692	0.99	33.9	
318 K	1490.7	0.714	0.99	98.38	
Langmuir					
		$Q_e = \frac{Q_m K_L C_e}{1 + K_L C_e}$			
T (K)	$K_L (\text{l/mg})$	$Q_m (\text{mg/g})$	R^2	CHI2	
288 K	0.106	7344.8	0.993	77.7	
303 K	0.165	7755.2	0.994	64.2	
318 K	0.228	8525.4	0.994	73.8	
Redlich–Peterson					
		$Q_e = \frac{K_R C_e}{1 + a_R C_e^\beta}$			
T (K)	$K_R (\text{l/g})$	$a_R (\text{l/mg})^{1/\beta}$	β	R^2	CHI2
288 K	925.97	0.2550	0.756	0.995	54.5
303 K	1411.75	0.2613	0.853	0.996	47.7
318 K	2017.75	0.2742	0.926	0.994	70.2
Thermodynamics parameters					
T (K)	$K_D \times 10^{-3} (\text{L/kg})$	$\Delta G^\circ (\text{kJ/mol})$	$\Delta H^\circ (\text{kJ/mol})$	$\Delta S^\circ (\text{kJ/mol K})$	
288 K	961.64	- 32.99	23.02	194.4	
303 K	1478.92	- 35.79			
318 K	2385.49	- 38.83			

in the present case. Actually, increasing temperature increases the kinetic energy of the DCL molecules due to which the activation energy barrier is conquered, and hence, intra-particle diffusion is increased. The coefficient of redetermination (R^2) value for all the isotherms (Freundlich, Langmuir and R–P) is very high ($R^2 \approx 0.99$) indicating all the isotherms are well representing the experimental data (Table 5). The Freundlich isotherm parameter K_F was also found increasing with temperature concluding higher adsorption at higher temperature. Higher n ($n > 1$) reflects the higher intensity of adsorption, which was also confirmed by the increasing value of Langmuir parameter, K_L , at increased temperature.

The Q_m in Langmuir isotherm representing the maximum adsorption capacity was found very high *i.e.*, 7344.8–8525.4 mg/g for temperatures 288–318 K (Table 5). In the literature available, the maximum 835.5 mg/g adsorption capacity towards doxycycline has been reported for adsorbent $\text{CoFe}_2\text{O}_4/\text{bio-silica}$ nanocomposite, [4, 29] In the present study, *nearly 10 times* higher adsorption capacity was observed for MCM-41 adsorbent. This indicates very high adsorption capability of MCM-41 towards DCL not only at higher temperature but at lower temperature also.

The ultimate isotherm models in terms of its calculated parameters at 303 K temperature (with least CHI2 error) is given in following form (Eqs. 13–15):

$$Q_e = 1100.3 (C_e^{0.692}) \text{ [Freundlich isotherm]} \quad (13)$$

$$Q_e = \frac{7755.2 \times 0.165 C_e}{1 + 0.165 C_e} \text{ [Langmuir Isotherm]} \quad (14)$$

$$Q_e = \frac{1411.75 C_e}{1 + (0.2613 C_e^{0.85})} \text{ [Redlich and Peterson Isotherm]} \quad (15)$$

Classical thermodynamics (Eq. 16) was applied to study the DCL – MCM-41 adsorption thermodynamics [51].

$$\ln K_D = \frac{-\Delta G^\circ}{RT} = \frac{\Delta S^\circ}{RT} - \frac{\Delta H^\circ}{R} \frac{1}{T} \quad (16)$$

where, T: Absolute temperature (K); R: Universal gas constant (8.314×10^{-3} kJ/mol.K); K_D (slope of $\ln(Q_e/C_e)$ versus Q_e): adsorption equilibrium constant; ΔG° : Gibbs free energy change (kJ/mol); ΔH° : change in enthalpy (kJ/mol); ΔS° : entropy change (J/mol K).

The calculated thermodynamics parameters (ΔG° , ΔS° and ΔH°) is represented in Table 5. ΔG° value was found negative at all the temperature indicating feasibility and spontaneity of DCL adsorption on MCM-41. Positive ΔS° indicated high randomness, high affinity of DCL towards MCM-41 with high degree of freedom of the DCL – MCM-41 system [52]. ΔH° of adsorption was found positive confirming the DCL adsorption on MCM-41 endothermic. The adsorption enthalpy for physisorption is 20 – 40 kJ/mol, whereas, for chemisorption, it is 80 – 240 kJ/mol. Therefore, $\Delta H^{\circ} = 23.02$ kJ/mol confirms the physisorption (as proposed in Sect. 3.3).

4 Conclusion

- Very high coefficient of determination (R^2) values 0.997 and 0.99 for %doxycycline removal and adsorption capacity, respectively, implied the validity of the model equation suggested by the Box Behnken Design to the experimental data.
- The maximum of the doxycycline is adsorbed on the MCM-41 at initial time of adsorption, which indicates high efficacy of the MCM-41.
- The optimum adsorption process parameters were found to be: $pH = 7.3$, adsorbent dose = 0.02 g/L and adsorption time = 20 min, and at this, the responses %doxycycline removal and adsorption capacity were, 99% and 2425 mg/g, respectively.
- Pseudo second-order kinetic model best suitably represented the adsorption kinetics data. Increasing trend of initial adsorption rate (h) and equilibrium adsorption capacity (Q_e) with increasing doxycycline concentration (C_o) concluded the adsorption is limited by the limiting C_o indicating high adsorption capacity of the MCM-41.
- Both the intra-particle and the surface diffusion was found controlling the adsorption process.
- The doxycycline adsorption on the MCM-41 was found endothermic, and all the isotherm model (Freundlich, Langmuir and R-P) are well representing the experimental data.
- In this study, maximum adsorption capacity for MCM-41 was observed to be 8525.4 mg/g, which is nearly 10 times higher than the adsorption capacity (835.5 mg/g) of CoFe₂O₄/bio-silica nanocomposite for doxycycline, reported in the literature.
- The interactions like hydrogen bonds between –OH and –H of doxycycline—MCM-41 adsorption system was found the probable mechanism of higher adsorption of DCL on MCM-41 surface. In zwitterionic form, the hydrophobic interaction of doxycycline with MCM-41 surface enhanced adsorption.

Acknowledgements Authors are thankful to the Department of Chemical Engineering, Thapar Institute of Engineering and Technology, Patiala, Punjab, India to provide Lab resources to conduct this work.

Declarations

Conflict of interest The authors report there are no competing interests to declare.

References

1. Klein EY, Boeckel TPV, Martinez EM, Pant S, Gandra S, Levin SA, Goossens H, Laxminarayan R (2018) Global increase and geographic convergence in antibiotic consumption between 2000 and 2015. *Proc Natl Acad Sci U S A* 115:E3463–E3470
2. Klein EY, Milkowska-Shibata M, Tseng KK, Sharland M, Gandra S, Pulcini C, Laxminarayan R (2020) Assessment of WHO antibiotic consumption and access targets in 76 countries, 2000–15: an analysis of pharmaceutical sales data. *Lancet Infect Dis*. [https://doi.org/10.1016/S1473-3099\(20\)30332-7](https://doi.org/10.1016/S1473-3099(20)30332-7)
3. The Center for Disease Dynamics, Economics & Policy (CDDEP) (2021) The State of the World's Antibiotics: A Global Analysis of Antimicrobial Resistance and Its Drivers
4. Aniagor CO, Igwegbe CA, Ighalo JO, Oba SN (2021) Adsorption of doxycycline from aqueous media: a review. *J Mol Liq* 334:116–124
5. McClain JBL, Ballou WR, Harrison SM, Steinweg DL (1984) Doxycycline therapy for leptospirosis. *Ann Intern Med* 100(5):696–698
6. Yates PA, Newman SA, Oshry LJ, Glassman RH, Leone AM, Reichel E (2021) Doxycycline treatment of high-risk COVID-19-positive patients with comorbid pulmonary disease. *Ther Adv Respir Dis* 14:1753466620951053
7. Hapeshi E, Fotiou I, Fatta-Kassinou D (2013) Sonophotocatalytic treatment of ofloxacin in secondary treated effluent and elucidation of its transformation products. *Chem Eng J* 224:96–105
8. WHO; Ten threats to global health in 2019 (2019) <https://www.who.int/news-room/feature-stories/ten-threats-to-global-health-in-2019>. Accessed 17 Apr 2020
9. Ding H, Wu Y, Zhang W, Zhong J, Lou Q, Yang P, Fang Y (2017) Occurrence, distribution, and risk assessment of antibiotics in the surface water of Poyang Lake, the largest freshwater lake in China. *Chemosphere* 184:137–147
10. Hu Y, Yan X, Shen Y, Di M, Wang J (2018) Antibiotics in surface water and sediments from Hanjiang River, Central China: occurrence, behavior and risk assessment. *Ecotoxicol Environ Saf* 157:150–158
11. Jiang Y, Xu C, Wu X, Chen Y, Han W, Gin KYH, He Y (2018) Occurrence, seasonal variation and risk assessment of antibiotics in Qingcaosha reservoir. *Water* 10(2):115
12. Baran W, Adamek E, Jajko M, Sobczak A (2018) Removal of veterinary antibiotics from wastewater by electrocoagulation. *Chemosphere* 94:381–389
13. Zaidi S, Chaabane T, Sivasankar V, Darchen A, Maachi R, Msagati T (2019) Electrocoagulation coupled electro-flotation process: feasible choice in doxycycline removal from pharmaceutical effluents. *Arab J Chem* 12(8):2798–2809
14. Zaidi S, Chaabane T, Sivasankar V, Darchen A, Maachi R, Msagati T, Prabhakaran M (2016) Performance efficiency of electrocoagulation coupled electroflotation process (EC-EF) versus adsorption process in doxycycline removal from aqueous solutions. *Proc Saf Environ Prot* 102:450–461

15. Ai X, Fan H, Wang Y, Guo Y, Liu X, Yang L, Liu H, Yang J (2018) XPS and Raman study of the active-sites on molybdenum disulfide nanopetals for photocatalytic removal of rhodamine B and doxycycline hydrochloride. *RSC Adv* 8(63):36280–36285
16. Bolobajev J, Trapido M, Goi A (2016) Effect of iron ion on doxycycline photocatalytic and Fenton-based autocatalytic decomposition. *Chemosphere* 153:220–226
17. Borghi A A, Silva MF, Al Arni S, Converti A, Palma MS (2015) Doxycycline degradation by the oxidative Fenton process. *J Chem* 2015:492030
18. Gao J, Gao Y, Sui Z, Dong Z, Wang S, Zou D (2018) Hydrothermal synthesis of BiOBr/FeWO₄ composite photocatalysts and their photocatalytic degradation of doxycycline. *J Alloy Compd* 732:43–51
19. Rivas J, Encinas A, Beltrán F, Graham N (2011) Application of advanced oxidation processes to doxycycline and norfloxacin removal from water. *J Environ Sci Health, Part A* 46(9):944–951
20. Hijosa-Valsero M, Fink G, Schlüsener MP, Sidrach-Cardona R, Martín-Villacorta J, Ternes T, Bécares E (2011) Removal of antibiotics from urban wastewater by constructed wetland optimization. *Chemosphere* 83(5):713–719
21. Kaur R, Kushwaha JP, Singh N (2018) Electrooxidation of ofloxacin antibiotic by dimensionally stable Ti/RuO₂ anode: evaluation and mechanistic approach. *Chemosphere* 193:685–694
22. Ighalo JO, Ajala JO, Umenweke G, Ogunniyi S, Adeyanju CA, Igwegbe CA, Adeniyi AG (2020) Mitigation of clofibric acid pollution by adsorption: a review of recent developments. *J Environ Chem Eng* 8(5):104264
23. Toor SK, Kushwaha JP, Sangal VK (2019) Adsorptive interaction of 4-aminobiphenyl with mesoporous MCM-41. *Phys Chem Liq* 57(6):720–732
24. Toor SK, Kushwaha JP, Sangal VK (2019) Aromatic amines equilibrium sorptive interaction with synthesized silica based mesoporous MCM-41: physicochemical evaluation and isotherm modelling. *J Environ Sci Health part A* 54(4):286–294
25. Li Y, Shang H, Cao Y et al (2022) High performance removal of sulfamethoxazole using large specific area of biochar derived from corncob xylose residue. *Biochar* 4:11
26. Liang H, Zhu C, Ji S et al (2022) Magnetic Fe₂O₃/biochar composite prepared in a molten salt medium for antibiotic removal in water. *Biochar* 4:3
27. Gao O, Shi W, Zhao M, Huang Z, Liu X, Ruan W (2022) Preparation of spiramycin fermentation residue derived biochar for effective adsorption of spiramycin from wastewater. *Chemosphere* 296:133902
28. Guo Y, Chen B, Zhao Y et al (2021) Fabrication of the magnetic mesoporous silica Fe-MCM-41-A as efficient adsorbent: performance, kinetics and mechanism. *Sci Rep* 11:2612
29. Olusegun SJ, Mohallem ND (2019) Insight into the adsorption of doxycycline hydrochloride on different thermally treated hierarchical CoFe₂O₄/bio-silica nanocomposite. *J Environ Chem Eng* 7(6):103442
30. Othman ZA (2012) A review: fundamental aspects of silicate mesoporous materials. *Materials* 5:2874–2902
31. Costa JAS, de Jesus RA, Santos DO, Mano JF, Romão LPC, Paranhos CM (2020) Recent progresses in the adsorption of organic, inorganic, and gas compounds by MCM-41-based mesoporous materials. *Microporous Mesoporous Mater* 291(1):109698
32. Cai Q, Luo ZS, Pang WQ, Fan YW, Chen XH, Cui FZ (2001) Dilute solution routes to various controllable morphologies of MCM-41 silica with a basic medium. *Chem Mat* 13:258–263
33. Moghaddam SS, Moghaddam AMR, Arami M (2010) Optimization through response surface methodology: coagulation/flocculation process for dye removal using sludge from water treatment plant. *J Hazard Mater* 175:651–657
34. Sangal VK, Kumar V, Mishra IM (2013) Optimization of a divided wall column for the separation of C₄–C₆ normal paraffin mixture using Box-Behnken design. *Chem Ind Chem Eng Q* 19:107–119
35. Aslan N, Cebeci Y (2007) Application of Box-Behnken design and response surface methodology for modeling of some Turkish coals. *Fuel* 86:90–97
36. Guven G, Perendeci A, Tanyolac A (2008) Electrochemical treatment of deproteinated whey wastewater and optimization of treatment conditions with response surface methodology. *J Hazard Mater* 157:69–78
37. Rossi A, Alves VA, Da Silva LA, Oliveira MA, Assis DOS, Santos FA, De Miranda RRS (2009) Electrooxidation and inhibition of the antibacterial activity of oxytetracycline hydrochloride using a RuO₂ electrode. *J Appl Electrochem* 39:329
38. Chao Y, Zhu W, Wu X, Hou F, Xun S, Wu P, Ji H, Xu H, Li H (2014) Application of graphene-like layered molybdenum disulfide and its excellent adsorption behavior for doxycycline antibiotic. *Chem Eng J* 243:60–67
39. Meziani MJ, Zajac J, Jones DJ, Rozie're J, Partyka S (2007) Surface characterization of mesoporous silicoaluminates of the MCM-41 Type: Evaluation of polar surface sites using flow calorimetry, adsorption of a cationic surfactant as a function of pore size and aluminum content. *Langmuir* 13:5409–5417
40. Kowalczuk D, Ginalska G, Golus J (2010) Characterization of the developed antimicrobial urological catheters. *Int J Pharm* 402:175–183
41. Kowalczuk D, Ginalska G, Przekora A (2011) The cytotoxicity assessment of the novel latex urinary catheter with prolonged antimicrobial activity. *J Biomed Mater Res Part A* 98A:222–228
42. Al-Ali AAS, Kassab-Bashi TY (2015) Fourier transform infra red (FTIR) spectroscopy of new copolymers of acrylic resin denture base materials. *IJERSTE* 4:172–180
43. Blanchard G, Maunaye M, Martin G (1984) Removal of heavy metals from water by means of natural zeolites. *Water Res* 18:1501–1507
44. Ho YS, McKay G (1999) Pseudo-second order model for adsorption processes. *Process Biochem* 34:451–465
45. Malik PK (2003) Use of activated carbons prepared from sawdust and rice-husk for adsorption of acid dyes: a case study of Acid Yellow 36. *Dyes Pig* 56:239–249
46. Kushwaha JP, Srivastava VC, Mall ID (2010) Treatment of dairy wastewater by commercial activated carbon and bagasse fly ash Parametric, kinetic and equilibrium modelling, disposal studies. *Biores Technol* 101:3474–3483
47. Rameshraj D, Srivastava VC, Kushwaha JP, Mall ID (2012) Quinoline adsorption onto granular activated carbon and bagasse fly ash. *Chem Eng J* 181–182:343–435
48. Ruthven DM (1984) Principles of adsorption and adsorption processes. Wiley, New York
49. Boyd GE, Adamson AW, Myers LS (1947) The exchange adsorption of ions from aqueous solutions by organic zeolites. *J Am Chem Soc* 69(11):2836–2848
50. Srivastava VC, Mall ID, Mishra IM (2007) Multi-component adsorption study of metal ions onto bagasse fly ash using Taguchi's design of experimental methodology. *Ind Eng Chem Res* 46:5697–5706
51. Srivastava VC, Mall ID, Mishra IM (2007) Adsorption thermodynamics and isosteric heat of adsorption of toxic metal ions onto bagasse fly ash (BFA) and rice husk ash (RHA). *Chem Eng J* 132(1–3):267–278
52. Mirzajani R, Pourreza N, Zayadi A, Malakooti R, Mahmoodi H (2015) Nanoporous calcined MCM-41 silica for adsorption and removal of Victoria blue dye from different natural water samples. *Desal Water Treat* 57(13):5903–5913